

https://doi.org/10.1070/QEL17375

Acousto-optic modulators of high-power laser radiation on the basis of KGW and KYW crystals

M.M. Mazur, L.I. Mazur, A.A. Sirotkin, A.V. Ryabinin, V.N. Shorin

Abstract. **Different modifications of acousto-optic modulators (AOMs) based on $KG(WO_4)_2$ (KGW) and $KY(WO_4)_2$ (KYW) crystals, designed for *Q* switching of high-power pulsed lasers, is developed and investigated. It is shown that AOMs based on these crystals are universal, can be combined with different lasers in the wavelength range of 1–3 μm, and have a high radiation resistance in the absence of antireflection coatings and light input at Brewster's angle. The operation efficiency of KGW-based AOMs is experimentally demonstrated. Solid-state lasers based on Cr:Er:YSGG (λ = 2.78 μm), Cr:Yb:Ho:YSGG (λ = 2.87 μm), Cr:Tm:Ho:YSGG (λ = 2.09 μm), and Nd:YAG (λ = 1.064 μm) crystals with active acousto-optic *Q* switching, operating in the repetitively pulsed regime with a high beam quality and without surface destruction, are investigated. Lasing pulses (30–60)-ns long with energy up to 32 mJ at a repetition rate from 1 to 1000 Hz are obtained.**

Keywords: *high-power solid-state IR lasers, acousto-optic modulators, KGW and KYW crystals.*

1. Introduction

Currently high-power solid-state *Q*-switched IR lasers, generating nanosecond pulses, are widely used for optical pumping of mid-IR coherent radiation sources, in biomedical applications, for remote sensing of atmospheric contaminants, etc.

Acousto-optic modulators (AOMs), which are based on laser beam diffraction from a volume grating formed by an acoustic wave [1], are used for *Q*-switching. The advantages of AOMs are simplicity and convenience in use; a relatively low cost; and a great variety of modifications, which allows one to choose an optimal version to solve a specific problem. AOMs are fabricated from crystals having low optical absorption at the lasing wavelength, high radiation resistance, and satisfactory acousto-optic quality. Up to date, the most popular AOM materials have been SiO_2 (quartz) and TeO_2 (paratellurite) crystals.

The crystals belonging to the family of double potassium tungstates $KMe(WO_4)_2$ (Me is a metal: Gd, Y, Yb, or Lu), which are also used in laser technologies, are efficient acousto-optic crystals. Due to their high radiation resistance [2] and transparency in a wide (0.4–3.5 μm) spectral range, they may serve a base for a series of acousto-optic devices aimed at controlling high-power laser beams [3]. Double potassium tungstates $KMe(WO_4)_2$ have close elastic and acousto-optic properties [3, 4] and optical characteristics [5–9]. An exception is the presence of a wide (0.8–1.1 μm) absorption band in the spectrum of $KYb(WO_4)_2$ crystal.

The characteristics of quartz, paratellurite, and $KGd(WO_4)_2$ crystals are listed in Table 1. The transmission spectra of $KGd(WO_4)_2$, paratellurite, and crystalline quartz are presented in Fig. 1.

Table 1. Characteristics of AOM materials.

Material	Transparency range/μm	Speed of sound/ 10^5 cm s^{-1}	Acousto-optic quality	Radiation resistance*/ GW cm^{-2}
SiO_2	0.2–2.7	6	1	20
TeO_2	0.35–4.5	4.3	20	0.25–0.30
$KGd(WO_4)_2$	0.35–3.5	4.3	6–10	20–170

*The radiation resistance of materials is indicated for 1.06-μm light and a pulse duration of 10 ns.

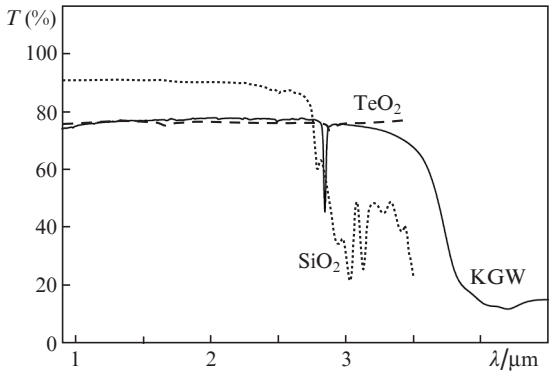

Figure 1. Transmission spectra of crystalline quartz (44-mm-thick), paratellurite (35 mm), and potassium--gadolinium tungstate (72 mm) samples.

An advantage of paratellurite is its high acousto-optic quality, which makes it possible to use low control powers and provides transparency in a wide (0.35–4.5 μm) spectral range; however, this material has a drawback: low radiation resistance. Quartz has a high radiation resistance [2], but low acousto-optic quality and unsatisfactory transmission at

M.M. Mazur, L.I. Mazur, A.V. Ryabinin, V.N. Shorin All-Russian Scientific Research Institute of Physical-Technical and Radiotechnical Measurements (VNIIFTRI), 141570 Mendeleevo, Moscow region, Russia; e-mail: ryabinin.nn@yandex.ru;
A.A. Sirotkin Prokhorov General Physics Institute, Russian Academy of Sciences, ul. Vavilova 38, 119991 Moscow, Russia

Received 29 May 2020
Kvantovaya Elektronika **50** (10) 957–961 (2020)
Translated by Yu.P. Sin'kov

wavelengths above 2.7 μm. The speed of sound in quartz is the highest, but its acousto-optic quality is lower than that of KGW by a factor of 6–10. To control an AOM based on a KGW crystal, one needs a high-frequency signal with a power an order of magnitude lower than that for quartz-based AOM. Correspondingly, even in simple cases, the cooling system for a KGW-based AOM should be simpler. For large light-beam apertures and radiation wavelengths above 2 μm, it may be impossible to design efficient quartz-based AOMs. In this case, AOMs based on KGW (or other $KMe(WO_4)_2$ crystals) may be irreplaceable.

Hence, neither quartz nor paratellurite have a complex of properties necessary for designing AOMs of high-power light in the range of 1–3 μm.

2. Analysis of the characteristics of AOMs based on KYW and KGW crystals

The acoustic and acousto-optic properties of $KMe(WO_4)_2$ crystals were investigated in a number of studies [3, 4, 10–14]. Using the matrices of elastic and photoelastic constants of these crystals, one can calculate the characteristics of AOMs implemented on these materials. Previously this calculation was performed for a KYW crystal in [15], where the characteristics of AOMs aimed at operating at a wavelength of 1.06 μm were investigated for two different propagation directions of ultrasonic wave (Table 2). Since KGW and KYW crystals have different properties, and the operation of a KYW-based AOM was considered in detail in [15], we believe if useful to analyse the specificity of the characteristics of KGW-based AOMs. It is of interest, because high-quality KGW crystals are more available than KYW crystals. When developing AOMs, one must know the acousto-optic efficiency M_2 for the chosen acoustic mode, the sound wave velocity, and the angle between the direction of sound-wave group velocity and its wave vector. One must also take into account the orientation of the permittivity ellipsoid axes relative to the propagation directions of light and sound beams. Figure 2 shows the corresponding parameters calculated for KGW and KYW crystals: the velocities of a quasi-longitudinal sound wave propagating in the Y plane of crystals, the angles between the wave vector and direction of group velocity, and the acousto-optic quality M_2 for light waves propagating along the $Y(N_p)$ axis, with polarisations directed along the N_g and N_m axes, as functions of the sound wave vector direction (N_p, N_g, and N_m are the principal axes of the refractive index ellipsoid of crystal).

In the Y plane of the KGW crystal, the acousto-optic efficiency M_2, determined by a quasi-shear wave propagating at an angle of –75° with respect to the N_g axis, is more than twice as high as the efficiency M_2 for the case of quasi-longitudinal acoustic wave [14]. Therefore, a more efficient AOM

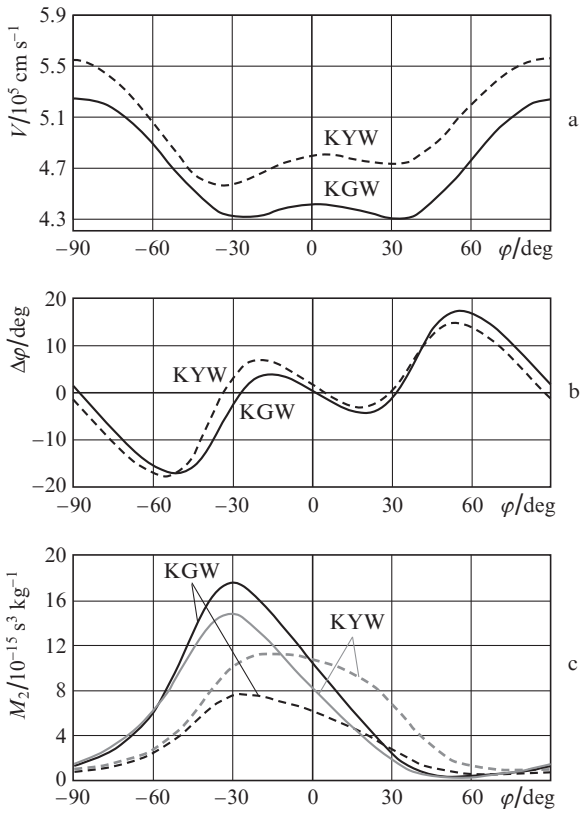

Figure 2. Dependences of (a) the quasi-longitudinal ultrasonic wave velocity V, (b) angle $\Delta\varphi$ between the group-velocity wave vector and direction, and (c) acousto-optic quality M_2 in the Y plane of KYW and KGW crystals for light waves propagating along the Y axis (N_p), with polarisations oriented in the N_g (solid lines) and N_m (dashed lines) directions, on the propagation direction of quasi-longitudinal sound wave, making an angle φ with the N_g axis.

can be implemented in this interaction configuration; however, the switching time is doubled, because the quasi-shear-wave velocity along the N_g axis is half of the quasi-longitudinal wave velocity.

The dependences presented in Figs 2b and 2c indicate that the angles between the directions of phase and group velocities are small, and the acousto-optic efficiency M_2 for the quasi-longitudinal wave propagating in the Y plane has maxima in the range of angles φ from 0 to –30°, which makes these ultrasonic wave propagation directions convenient for use in AOMs.

The maximum values of acousto-optic efficiency for both crystals are provided for a light wave propagating along the Y axis, with polarisation directed along the N_g axis, if a quasi-longitudinal sound wave propagates in the Y plane, making

Table 2. Characteristics of KYW- and KGW-based AOMs.

Characteristic	KYW			KGW	
Light wavelength/μm	0.63	2.1	2.8	1.064	1.064
Converter size/mm	25 × 2.5	48 × 3	48 × 3	25 × 2.5	29 × 2.5
Diffraction efficiency/% W^{-1}	55 ($\varphi = 0$, N_g) 40 ($\varphi = 0$, N_m) 74 (–30°, N_g) 40 (–30°, N_m)	11 (–30°, N_g) 8.5 (–30°, N_m)	4.5 (–30°, N_g)	36 ($\varphi = 0$, N_g) 25 ($\varphi = 0$, N_m)	62 (–30°, N_g) 38 (–30°, N_m)

an angle $\varphi \approx -30°$ with the N_g axis. Under these conditions, the acousto-optic efficiency M_2 of the KGW crystal somewhat exceeds that for the KYW crystal. For a sound wave propagating at an angle $\varphi \approx -12°$ with respect to the N_g axis in a KYW crystal, the acousto-optic efficiency is the same for both polarisations, due to which such orientation can be used to design an efficient polarisation-insensitive AOM. A number of AOMs based on KGW and KYW crystals with sound wave propagating at angles $\varphi \approx 0$ and $-30°$ with respect to the N_g axis were developed, fabricated, and tested. The working frequency of ultrasonic converters in these AOMs is 50 ± 10 MHz, which provides the Bragg diffraction conditions. The modulators work in the travelling-wave regime. Their characteristics are listed in Table 2.

Some of the aforementioned AOMs are successfully used for Q switching of lasers generating at wavelengths of 2.1 and 2.8 μm [16, 17]. However, degradation of antireflection coatings (when high-power pulses were generated) was revealed during exploitation of these modulators.

3. Brewster AOM based on a KGW crystal

The AOM radiation resistance is often limited by the antireflection-coating damage thresholds. This is especially urgent when designing an AOM of high-power light in the wavelength range in the vicinity of ~3 μm, where one meets problems with deposition of antireflection coatings having high damage thresholds.

Introducing radiation into an AOM at Brewster's angle, one can increase the AOM radiation resistance up to the value typical of the crystal. However, an additional problem arises in this case. An AOM in which a light beam enters the crystal at Brewster's angle can deal with only linearly polarised radiation, because reflection losses are very high at other polarisations. A laser beam, being introduced into the AOM at a Brewster angle, broadens proportionally to the refractive index of crystal [by a factor of about two for $KMe(WO_4)_2$]. If the input face in the Brewster AOM is oriented parallel to the sound wave vector, this configuration provides (at a specified acousto-optic diffraction efficiency) an increase in the required power of high-frequency driving generator proportionally to the refractive index. If the input face in the Brewster AOM is parallel to the vector oriented perpendicular to the wave vectors of light and sound waves, the AOM switching time increases proportionally to the refractive index. To maintain the switching time constant, the input face in all fabricated Brewster AOMs was oriented parallel to the sound wave vector, i.e., perpendicular to the ultrasonic converter plane.

The displacement of a beam introduced at Brewster's angle and transmitted through one cell is $\Delta = L(n_m^2 - 1) \times (n_m^2 + 1)^{-1}$, where n_m is the refractive index. The laser beam is returned to the initial position using additional prism *2*, which is a mirror image of acousto-optic cell *1* (Fig. 3).

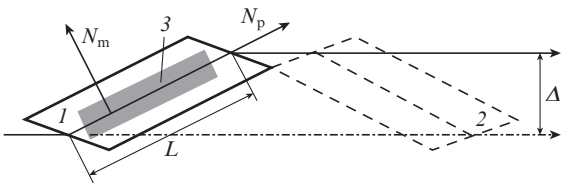

Figure 3. Schematic of an AOM with a light beam introduced at Brewster's angle: (*1*) acousto-optic cell; (*2*) correcting prism; (*3*) ultrasonic converter; L is the length of acousto-optic cell and Δ is the displacement of the optical beam transmitted through one cell.

We fabricated two AOM versions, where an optical beam is introduced at Brewster's angle. In one of them, we used one cell, and the beam underwent a spatial displacement. In the other one, we applied a scheme reconstructing the optical beam spatial position, as shown in Fig. 3. The characteristics of a KGW-based Brewster AOM are given in Table 3.

Both AOM versions demonstrated their operability. Since the refractive index dispersion in $KMe(WO_4)_2$ crystals is small in the spectral range of 1–3 μm [6–9] and there are no antireflection coatings, the aforementioned AOM designs can successfully operate in a wide spectral range. A convenient feature of the two-cell AOM version is as follows: when inserting this modulator in the laser cavity, one barely needs to tune the cavity. However, the presence of the second cell increases the intracavity loss; in addition, this AOM is more complicated and expensive.

To demonstrate the potential of the universal AOM based on a KGW crystal, we tested it using nanosecond lasers with working wavelengths varying in a wide range: from 1 to 3 μm.

A schematic of the experimental bench is presented in Fig. 4. The cavity was formed by a highly reflecting mirror M1 with a dielectric coating having a high reflectance at the laser wavelength and a flat output mirror M2 with a partially reflecting dielectric coating (reflectance of ~50%–75%) in the wavelength range of 1–3 μm. The total laser cavity length was 325 mm. The single-mode regime of generating output radiation was achieved using a diaphragm 1.5–2 mm in diameter, which was installed in the cavity.

An AOM based on a KGW crystal was placed in the cavity near the highly reflecting mirror. One AOM sample was

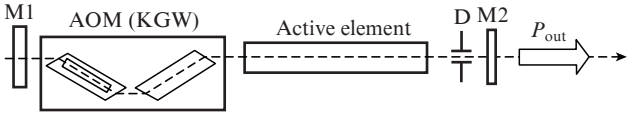

Figure 4. Schematic of the experimental bench: (M1, M2) cavity mirrors; (D) diaphragm; active element: Nd:YAG (3 × 120 mm), Cr:Tm:Ho:YSGG (5 × 100 mm), Cr:Er:YSGG (5 × 100 mm), or Cr:Yb:Ho:YSGG (4.5 × 95 mm) crystals.

Table 3. Characteristics of a KGW-based Brewster AOM.

Converter size	Light beam diameter	Diffraction efficiency		
		1.06 μm	2.1 μm	2.8 μm
42 × 3 mm	1.5 mm	64% (W = 2.2 W)	70% (W = 12 W)	56% (W = 33 W)

Note: W is the high-frequency signal power at the AOM input.

used for operation in the wavelength range of 1–3 μm. The modulator consisted of two parts (active and passive), 45 mm in size. Its external faces were oriented at Brewster's angle (see Fig. 4). The passive part made it possible to compensate for the beam displacement in the cavity. The modulator was controlled using a GSN 50-30 sinusoidal voltage generator with a maximum high-frequency signal power of 30 W. The temporal laser characteristics were measured by a PVM-10.6 photodiode (Vigo System) with a temporal resolution $\tau \approx 1$ ns and a GW Instek GDS-73154 oscilloscope. The energy was measured by a pyroelectric Ophir detector.

Four laser crystals were used to test AOMs at wavelengths in the range from 1 to 3 μm: Cr:Er:YSGG (λ = 2.78 μm), Cr:Yb:Ho:YSGG (λ = 2.87 μm), Cr:Tm:Ho:YSGG (λ = 2.09 μm), and Nd:YAG (λ = 1.064 μm).

When studying the modulator at a wavelength of 1.064 μm, a diode side-pumped laser module RD40 (Northrop Grumman) based on an Nd:YAG crystal (3 mm in diameter, 120 mm long) served as an active medium. The end faces of the active element had antireflection coatings at the lasing wavelength. The laser operated in the active Q-switching regime. The cavity was formed by a highly reflecting mirror M1 (radius of 500 mm) with a dielectric coating having a high reflectance at a wavelength of 1.064 μm and a flat output mirror M2 with a dielectric coating having a reflectance of ~70%. At a pulse repetition rate of 1 kHz, 30-ns pulses with energy up to 12 mJ were obtained.

A lamp-pumped laser based on Cr:Tm:Ho:YSGG crystal was used to test the AOM at a wavelength of 2.09 μm. The active element had a diameter of 5 mm and a length of 100 mm; its end faces had no antireflection coatings. The cavity was formed by a highly reflecting plane mirror M1 with a dielectric coating having a high reflectance at a wavelength of 2.09 μm and flat output mirror M2 with a dielectric coating having a reflectance of ~75%. The laser generated 60-ns pulses with energy up to 28.5 mJ at a repetition frequency of 3 Hz.

Of greatest interest were the investigations aimed at designing a solid-state 3-μm Q-switched laser (operating in the repetitively pulsed regime) in order to implement the highest energetic parameters. Specifically in this spectral range AOMs of this type come into their own.

An YSGG:Cr:Er crystal 5 mm in diameter and 100 mm long was used as an active medium (without antireflection coatings on the end faces), emitting in the vicinity of λ = 2.78 μm on the $^4I_{11/2} \rightarrow {}^4I_{13/2}$ transition of erbium ions. We also investigated a solid-state laser working on the $^5I_8 \rightarrow {}^5I_6$ transition of Ho^{3+} ions in Cr:Yb:Ho:YSGG (λ = 2.87 μm), with acousto-optic Q switching. The active element based on a Cr:Yb:Ho:YSGG crystal had a length of 95 mm and a diameter of 4.5 mm.

The laser cavity was formed by two flat mirrors, M1 and M2, with reflectances of ~100% and 60%, respectively. The active element and pump lamp were located in a quantron and cooled with water. The quantron temperature was maintained at a level of ~18 °C. The xenon lamp pump pulse was ~200 μs long. Under these conditions, stable lasing was maintained at a pulse repetition rate up to 10 Hz. The output radiation was linearly polarised because the modulator had Brewster faces. A maximum output energy of 32 mJ was obtained with a Cr:Er:YSGG crystal at a wavelength of 2.78 μm. The measured lasing pulse duration was ~60 ns (Fig. 5).

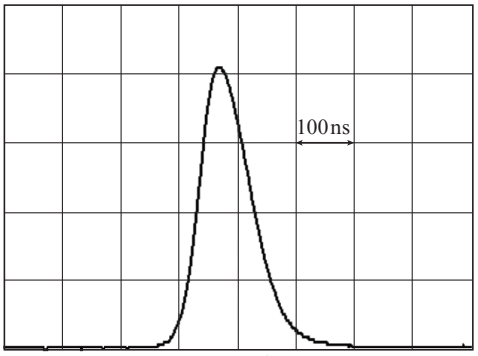

Figure 5. Oscillogram of an YSGG:Cr:Er laser pulse (λ = 2.78 μm), obtained in the Q-switching regime at a pulse repetition rate of 2–10 Hz.

Thus, the developed lasers based on Cr:Er:YSGG and Cr:Yb:Ho:YSGG crystals, operating in the Q-switching regime, provide stable generation of megawatt power in both multimode and single-mode regimes and can successfully be applied in different fields.

4. Conclusions

Different modifications of AOMs based on KGW and KYW crystals, designed for Q switching of high-power pulsed lasers operating in the spectral range of 1–3 μm, were developed and investigated.

The AOMs based on KGW and KYW crystals have no alternative in the case of high-power lasers generating at wavelengths exceeding 2 μm. The AOMs on the basis of these crystals, with light introduced at Brewster's angle, have no limitations on light power determined by the radiation resistance of antireflection coatings. Due to the small refractive index dispersion, they can operate at any wavelength in the range of 1–3 μm.

The operation efficiency of a universal KGW-based AOM was experimentally demonstrated. Solid-state lasers based on Cr:Er:YSGG (λ = 2.78 μm), Cr:Yb:Ho:YSGG (λ = 2.87 μm), Cr:Tm:Ho:YSGG (λ = 2.09 μm), and Nd:YAG (λ = 1.064 μm) crystals with active acousto-optic Q switching, operating in the repetitively pulsed regime with high beam quality and without surface damage, were investigated.

Acknowledgements. We are grateful to A.A. Pavlyuk for fruitful cooperation. All crystals used to design AOMs and described in this paper were synthesised under his guidance at the Nikolaev Institute of Inorganic Chemistry, Siberian Branch, Russian Academy of Sciences. We are also grateful to A.V. Pushkin for measuring the AOM diffraction efficiency at 2.8 μm.

References

1. Tarasov L.V. *Fizika protsessov v generatorakh kogerentnogo opticheskogo izlucheniya* (Physics of Processes in Generators of Coherent Optical Radiation) (Moscow: Radio i Svyaz', 1981).
2. Mochalov I.V. *Opt. Eng.*, **36** (6), 1660 (1996).
3. Mazur M.M., Velikovskiy D.Yu., Mazur L.I., Pavluk A.A., Pozhar V.E., Pustovoit V.I. *Ultrasonics*, **54**, 1311 (2014); http://dx.doi.org/10.1016/j.ultras.2014.01.009.
4. Mazur M.M., Mazur L.I., Pozhar V.E. *Ultrasonics*, **73**, 231 (2017).

5. Mateos X., Sole R., Gavalda Jna., Aguilo M., Massons J., Diaz F. *Opt. Mater*., **28**, 423 (2006).
6. Kaminskii A.A., Konstantinova A.F., Orekhova V.P., Butashin A.V., Klevtsova R.F., Pavlyuk A.A. *Crystallogr. Rep*., **46** (4), 665 (2001).
7. Pujol M.C., Rico M., Zaldo C., Sole R., Nikolov V., Solans X., Aguilo M., Dıaz F. *Appl. Phys. B*, **68** (2), 187 (1999).
8. Pujol M.C., Barsukova M., Guell F., Mateus X., Sole R., Gavalda Jna., Aguilo M., Massons J., Dıaz F., Klopp P., Grieber U., Petrov V. *Phys. Rev. B*, **65**, 165121 (2002); http://prb.aps.org/abstract/PRB/v65/i16/e165121.
9. Pujol M.C., Mateus X., Aznar A., Solans X., Surinach S., Massons J., Dıaz F., Aguilo M. *Appl. Crystallogr*., **39**, 230 (2006). DOI: 10.1107/S0021889806004328.
10. Mazur M.M., Mazur L.I., Kuznetsov F.A., Pavlyuk A.A., Pustovoit V.I. *Inorg. Mater*., **48** (1), 67 (2012).
11. Mazur M.M., Velikovskii D.Yu., Kuznetsov F.A., Mazur L.I., Pavlyuk A.A., Pozhar V.E., Pustovoit V. *Acoust. Phys*., **58** (6), 658 (2012).
12. Mazur M.M., Mazur L.I., Pozhar V.E. *Pis'ma Zh. Tekh. Fiz*., **41** (5), 91 (2015).
13. Velikovskii D.Yu., Mazur M.M., Pavlyuk A.A., Pozhar V.E., Solodovnikov S.F., Yudanova L.I. *Phys. Wave Phenom*., **23** (1), 58 (2015).
14. Mazur M.M., Mazur L.I., Pozhar V.E. *Phys. Procedia*, **70**, 741 (2015).
15. Mazur M.M., Mazur L.I., Pozhar V.E., Shorin V.N., Konstantinov Yu.P. *Quantum Electron*., **47** (7), 661 (2017) [*Kvantovaya Elektron*., **47** (7), 661 (2017)].
16. Sirotkin A.A., Mazur M.M. *Proc. 2018 Int. Conf. on Laser Optics (ICLO)* (St.Petersburg, 2018) p. 46.
17. Pushkin A.V., Mazur M.M., Sirotkin A.A., Firsov V.V., Potemkin F.V. *Opt. Lett*., **44**, 4837 (2019).